

Thermal degradation and stability of epoxy nanocomposites: Influence of montmorillonite content and cure temperature

F. Carrasco^{a,*}, P. Pagès^b

^a Department of Chemical Engineering, Universitat de Girona, Campus Montilivi, s/n. 17071 Girona, Spain

^b Department of Material Science, Universitat Politècnica de Catalunya, C/Colom 11. 08222 Terrassa, Spain

Received 26 November 2007; received in revised form 21 December 2007; accepted 14 January 2008

Available online 26 January 2008

Abstract

The thermal behaviour and stability of epoxy nanocomposites were studied by thermogravimetric analysis (TGA). The nanocomposites consisted of a trifunctional epoxy resin, a hardener containing reactive primary amine groups and clay nanoparticles (i.e. montmorillonite), previously treated with octadecyl ammonium. Three levels of nanoclay content (0, 5 and 10%) and three temperature levels (120, 150 and 200 °C) were used. The exfoliation of nanoparticles within the material was analyzed by X-ray diffraction (XRD). The cure conversion was determined by Fourier transform infrared (FTIR) spectroscopy by selecting the suitable band for epoxide functional groups. The study demonstrated that the nanoclay greatly accelerates the cure, at the different cure temperatures studied. Finally, the thermal stability of the various nanocomposites was established by calculating various characteristic temperatures from thermograms as well as conversion and conversion derivative at maximum decomposition rate. The collisions between resin molecules, which are trapped within the nanoclay galleries, were less effective because they were protected against thermal degradation by the galleries. However, once the collision was effective, the thermal activation occurred more readily.

© 2008 Elsevier Ltd. All rights reserved.

Keywords: Thermal degradation; Activation energy; Nanogalleries; Nanoclay content; Cure temperature

1. Introduction

Polymer-based nanocomposites consist of thermoset, thermoplastic or elastomeric matrices reinforced with nanoparticles or nanofibres. These materials are of great interest from an industrial and scientific perspective because they show much better behaviour and characteristics in comparison with conventional composites [1–9]. A new generation of multifunctional epoxy resins (with a level of functionality of 3–5) had a great impact on the market because their properties were better than those of earlier conventional (i.e. bifunctional) epoxy resins [10]. At the same cure level, multifunctional resins have better crosslink densities and glass transition temperatures, providing a considerable increase in

their thermal, dynamic, mechanical and adhesive properties in comparison with their bifunctional predecessors [11,12]. The resin used in this work was a trifunctional resin derived from *p*-aminophenol, and it is notable for its low viscosity (which facilitates nanocomposite manufacturing) and its excellent hardness and mechanical behaviour, which are maintained at high temperatures.

Epoxy resin reinforced with nanoscopic layered silicates has received increasing attention recently because of the possibility of obtaining improved properties in terms of stiffness, strength, fire resistance, dimensional stability and shrinkage [13]. Hydrophilic clay is not highly compatible with the epoxy matrix. To improve their interfacial interaction, surface modification of the nanoclay by organic compounds, known as intercalants, is essential. The effect of the intercalant on the polymerization of epoxy has been previously reported, but only few investigations have been carried out on its influence on the mechanism and kinetics of cure [14,15], as well as on

* Corresponding author. Tel.: +34972418461; fax: +34972418399.

E-mail address: felix.carrasco@udg.edu (F. Carrasco).

the relationship between cure conditions and thermal stability. In addition, it is important to consider the steric effect of nanoclay on the cure of intercalated material, as previously described [16,17]. There is competition between diffusion of hardener molecules into the clay galleries and cure reactions between the hardener and epoxy outside the galleries. It has to be noted that FTIR is a technique widely used to evaluate the conversion of functional groups present in polymer materials, thus leading to the quantification of various types of transformations within their chemical and physical structure (i.e. aging of polymers, interactions in polymer composites, crystallinity, and cure of resins and composites, among others) [18–21].

The thermal degradation and stability of resins (in the presence or not of fillers and nanofillers) as well as other polymer materials have been studied by various techniques, such as X-ray diffraction (XRD), scanning electron microscopy (SEM), differential scanning calorimetry (DSC), thermogravimetric analysis (TGA), dynamic mechanical thermal analysis (DMTA), FTIR spectroscopy and high-resolution pyrolysis-gas chromatography, among others [22–30]. These works analyzed the thermal degradation from different points-of-view: determination of activation energies, glass transition temperature, conversion, rate, thermal stability, enthalpy changes as well as identification of products.

The aim of this work was to study the effect of nanoclays (i.e. montmorillonite) on the cure rate and thermal degradation and stability of epoxy nanocomposites. The thermal stability of cured materials was studied as a function of cure temperature and nanoclay content by means of thermogravimetric analysis (TGA). The cure conversion was monitored by FTIR spectroscopy by following the disappearance of epoxide functional groups.

2. Materials and methods

2.1. Materials

An organo-nanoclay recommended for amine-cured epoxy resins, Nanomer I30E from Nanocor Inc. (Arlington Heights, Illinois, USA), with particle length ranging between 100 and 150 nm and thickness of approximately 1 nm, was used in this study. It consists of montmorillonite treated with octadecylamine, a primary amine base. The matrix was a trifunctional epoxy resin (TGAP), marketed as Araldite MY510 from Vantico, with a viscosity at 25 °C of 0.55–0.85 Pa s, density of 1205–1225 kg/m³ and a maximum moisture content of 0.20%. The hardener used was 4-4'-diaminodiphenylsulfone, marketed as HT-976-1, from Vantico. All materials were used without further purification.

2.2. Nanocomposite preparation

The mixture of resin and nanoclay was prepared in the appropriate quantities in order to obtain materials with the desired proportion of nanoparticles (0, 5 and 10%, by mass) and mixed by hand for 2 min. The mixture was then placed

in an ultrasound bath for 1 h in order to ensure correct dispersion. The mixture was then heated to 80 °C. This temperature was maintained while the hardener was slowly added. The mixture was then stirred for 20 min. The ratio of resin to hardener, by mass, was 100/52, which corresponds to a slight excess of primary amine groups with respect to the epoxide groups present in the resin. In order to prepare the material correctly, it was essential to remove the entrapped air by placing it in a vacuum oven until all bubbles were seen to be gone from the mixture. Then, small amounts of the above mixtures (200 mg) were deposited on NaCl crystals. Once they were in the oven, their FTIR spectra were recorded, at the selected temperature (120, 150 or 200 °C), every 10 min until the treatment had completely finished. All samples were pre-cured (30 min at 50 °C and 30 min at 100 °C, reaching in these conditions conversions as low as 4–6%) in order to avoid deflagrations during the cure process. Cure conversions were corrected to take into consideration the conversion reached during the pre-cure period.

2.3. Instrumental techniques

To evaluate the exfoliation of the nanoclay into the polymer matrix, X-ray diffraction patterns were obtained by using a Bruker D8 Advance powder diffractometer with Cu K α radiation ($\lambda = 1.5406$ Å, power = 40 kV, $2\theta = 20^\circ$).

A Nicolet 510 M spectrophotometer was used for obtaining FTIR spectra in the wavenumber range of 4000–750 cm⁻¹. The cure process was studied by evaluating the decrease of the specific band of the epoxide groups at 906 cm⁻¹. This is the most suitable as it does not overlap with other peaks. The band of the benzene ring, which appears at 1513 cm⁻¹, was chosen as an invariant reference band and was used to calculate the reduced absorbance.

TGA data were obtained on a Mettler Toledo thermogravimetric analyzer, model TG50-M3. The samples were heated at 10 °C/min from room temperature to 600 °C, under a dry nitrogen gas flow rate of 200 mL/min.

3. Results and discussion

3.1. Nanoparticle exfoliation

The dispersion of nanoparticles within the material was previously studied by means of optical microscopy with polarized light and also by TEM and SEM. The results showed that there was a good dispersion and there was no formation of aggregates. Moreover, XRD analysis was carried out on various zones of each sample and results proved to be reproducible. X-ray diffraction plots of the Nanomer I30E clay, the uncured epoxy–nanoclay system, the cured resin without nanoclay and the cured nanocomposite with 5% of nanoclay (both cured at 200 °C for 3 h) are illustrated in Fig. 1. An intense peak at $2\theta = 4.2^\circ$ was observed for the crystalline montmorillonite, which totally disappeared when the nanoparticles were dispersed within the cured material, whereas a small peak remained for the uncured material. Therefore, the results

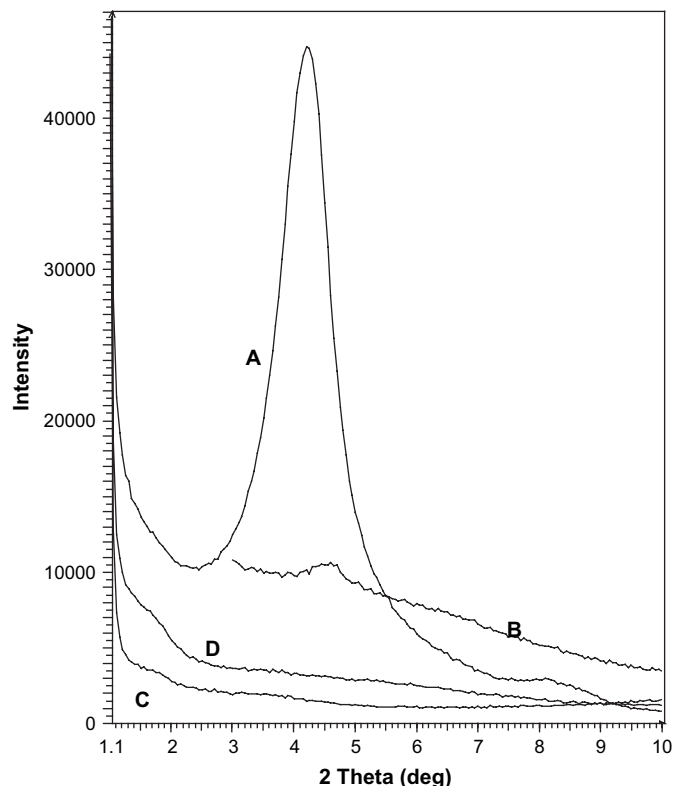


Fig. 1. X-ray diffraction for: (A) nanoclay I.30E; (B) uncured resin with 5% of nanoclay; (C) cured resin at 200 °C for 3 h; and (D) cured material (with 5% of nanoclay) at 200 °C for 3 h.

clearly show that the nanoparticles were fully exfoliated into the epoxy matrix of the cured materials, but the exfoliation was not complete when the cure agent was not added. This indicated that the cured systems were thermodynamically stable at all cure temperatures.

3.2. Study of cure reactions by FTIR spectroscopy

Curing was studied by evaluating the decrease of the specific band of the epoxide functional groups. Thus, for each of the nanocomposites obtained, the progress in the curing reaction was followed by calculating the curing conversion, $\alpha = 1 - A(t)/A(0)$, where $A(t)$ and $A(0)$ are the reduced absorbances at time t and at starting time, respectively, corresponding to the aforementioned vibration band of the epoxide group at 906 cm^{-1} . The band of the benzene ring, which appears at 1513 cm^{-1} , was chosen as an invariant reference band and was used to calculate the reduced absorbance for epoxide functional groups.

Figs. 2–4 show the variation of epoxide conversion as a function of cure time and temperature (120, 150 and 200 °C, respectively) for materials containing 0, 5, and 10% of nanoclay. As shown in Table 1, there was an asymptotic conversion value, depending on both cure temperature and nanoclay content: 75–80%, 85–92% and 99–100%, when curing at 120, 150 and 200 °C, respectively. Therefore, cure asymptotic conversions increased when increasing

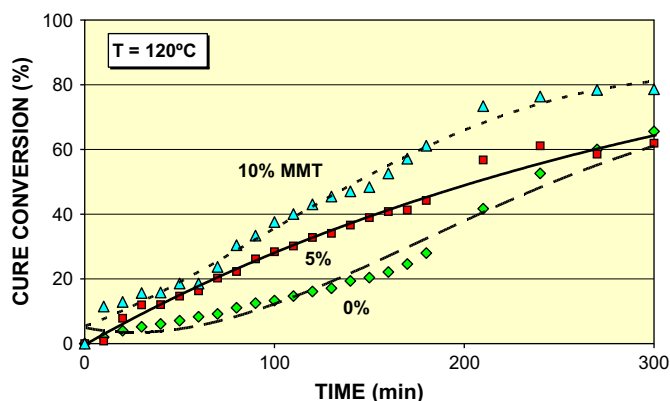


Fig. 2. Variation of cure conversion as a function of time for materials (containing 0, 5 and 10% of nanoclay) cured at 120 °C.

temperature at a given nanoclay content. On another hand, at a given temperature, it was also demonstrated that asymptotic cure conversions also increased when increasing nanoclay content (from 0 to 5%). It is relevant to emphasize that total cure was reached at 200 °C, independently on the presence or absence of nanoparticles. Asymptotic values of conversion were also previously reported [10] when curing the same epoxy resin without the presence of nanoparticles. Only at the highest temperature (i.e. 200 °C), it was possible to attain the total nanocomposite cure. Therefore, there was a barrier effect at lower temperatures, not allowing the progression of cure reactions, as previously reported [15].

During the initial stages of cure, temperature and nanoclay content had a very significant influence on cure rate. Indeed, during the first 40 min, the mean reaction rate at 120 °C was 0.15, 0.30 and 0.40%/min for nanoclay content of 0, 5 and 10%, respectively. On another hand, the mean reaction rate at 150 °C was 0.50, 1.66 and 1.97%/min, and finally, the mean reaction rate at 200 °C was 2.21, 2.26 and 2.27%/min. Therefore, the mean reaction rate during this period of time increased significantly when increasing the cure temperature for each nanoclay content and also increased when increasing the nanoclay content at a given temperature (with the exception of curing at 200 °C, being the mean reaction rate independent of

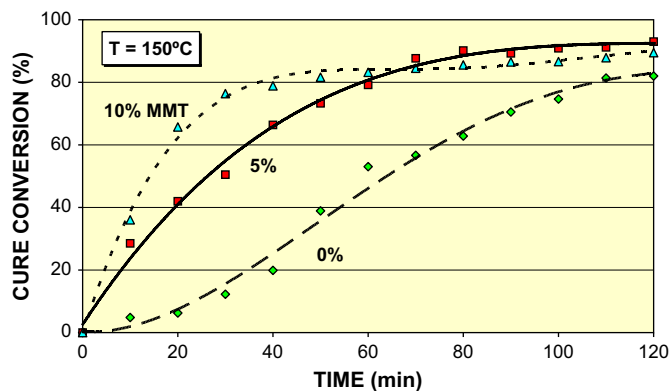


Fig. 3. Variation of cure conversion as a function of time for materials (containing 0, 5 and 10% of nanoclay) cured at 150 °C.

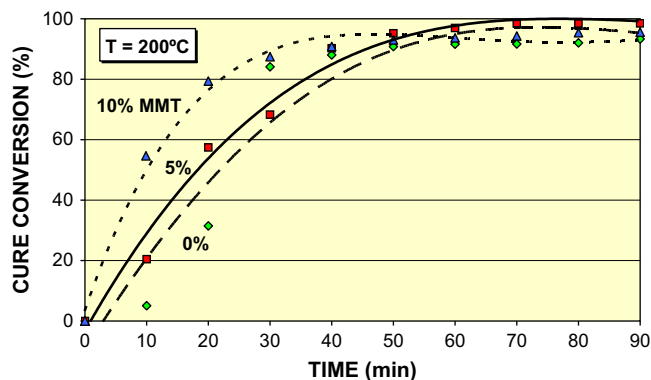


Fig. 4. Variation of cure conversion as a function of time for materials (containing 0, 5 and 10% of nanoclay) cured at 200 °C.

the nanoclay content). The asymptotic value of conversion was reached at 270–450 min (at 120 °C), 110–140 min (at 150 °C) and 50–70 min (at 200 °C), depending on the nanoclay content (the higher the nanoclay content, the lower the cure time). These results clearly showed that cure at 120 °C took place slowly whereas cure at temperatures of 150 or 200 °C was completed at lower time. For this reason, Fig. 5 was plotted in order to visualize how the presence of nanoparticles led to faster cure of materials. Indeed, after 30 min, the cure conversion of resin (0% of nanoclay) at 150 °C was of 12%, whereas the cure of nanocomposite (10% of nanoclay) at 200 °C was very high, with a cure conversion of 88%. These findings demonstrate and confirm that the surface modifier (octadecyl ammonium) of the nanoclay accelerates the cure process, as previously reported [7]. These authors demonstrated that acidic onium ions (i.e. acidic cations) of diamines catalyze the intragallery epoxide polymerization process. The higher reactivity of the ammonium surface modifier explains why a greater proportion of nanoclay in the nanocomposite increases the epoxide conversion during the initial cure stages. As it has been previously reported [31], the process starts with the reaction of the primary amine which is usually completed by about conversion of 60%, and this is accompanied

Table 1
Values of asymptotic conversion (α_m) as a function of nanoclay content at three cure temperature levels

| Nanoclay content (%) | α_m (%) |
|----------------------|----------------|
| <i>T</i> = 120 °C | |
| 0 | 74.8 |
| 5 | 80.0 |
| 10 | 80.0 |
| <i>T</i> = 150 °C | |
| 0 | 85.2 |
| 5 | 93.3 |
| 10 | 92.2 |
| <i>T</i> = 200 °C | |
| 0 | 98.7 |
| 5 | 100 |
| 10 | 99.4 |

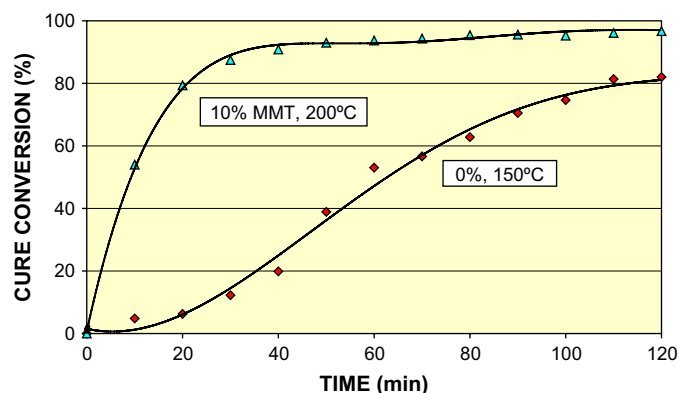


Fig. 5. Comparison of conversion for curing resin (0% of nanoclay) at 150 °C and nanocomposite (10% of nanoclay) at 200 °C.

by the reaction of the secondary amine which continues until about conversion of 80%. Finally, and generally towards the end of the cure process, there is etherification via the secondary amine, catalyzed by the tertiary amines, as well as etherification via cationic homopolymerization initiated by the onium ion of the organically modified nanoclay. These various reactions are not sequential, but can instead occur simultaneously over a certain range of conversion.

Another way to study the cure rate consists of evaluating half-life ($t_{1/2}$) values. Indeed, Table 2 shows the variation of this parameter with cure temperature and nanoclay content. In all cases, half-life decreased when increasing cure temperature and nanoclay content. The results clearly indicated that cure must be conducted at 150 or 200 °C, because 120 °C was too low (i.e. half-life values were very high, between 113 and 208 min). Table 2 contains relevant data, showing that it was possible to attain similar half-life values at lower temperatures by incorporating nanoparticles (i.e. half-life values equal to 22–24 min were reached with the following operating conditions: 150 °C and 5% of nanoclay, and 200 °C without nanoclay). Cure reactions were very fast when operating at 200 °C for materials containing 10% of nanoclay (i.e. $t_{1/2}$ = 10 min).

Table 2
Values of cure half-life ($t_{1/2}$) as a function of nanoclay content at three cure temperature levels

| Nanoclay content (%) | $t_{1/2}$ (min) |
|----------------------|-----------------|
| <i>T</i> = 120 °C | |
| 0 | 208.0 |
| 5 | 153.5 |
| 10 | 113.0 |
| <i>T</i> = 150 °C | |
| 0 | 56.8 |
| 5 | 24.0 |
| 10 | 12.6 |
| <i>T</i> = 200 °C | |
| 0 | 21.8 |
| 5 | 18.4 |
| 10 | 10.0 |

3.3. Study of thermal degradation and stability by thermogravimetric analysis

The thermal degradation and stability of the different materials were studied by thermogravimetric analysis (TGA). Various temperatures related to the thermal stability can be determined from TGA data: T_5 , T_{50} and T_{95} , defined as temperature at which 5, 50 and 95% of the mass is volatilized, respectively. In fact, T_5 provides a good idea of the thermal stability. It has to be noted that the quantification of the beginning of the thermal decomposition (i.e. conversions near to 0) is very difficult, because low conversion variations in this zone correspond to high temperature variations. Because of the high mineral content of montmorillonite (70%) and char formation due to degradation under nitrogen atmosphere, it was not possible to evaluate T_{95} for the nanocomposites.

Figs. 6 and 7 show the variation of the thermal degradation conversion (α) and conversion derivative ($d\alpha/dT$), respectively, as a function of temperature for uncured resin and materials cured at 200 °C for 3 h (at three levels of nanoclay content: 0, 5 and 10%). Conversion was calculated with respect to the initial total sample mass. These figures clearly illustrated that the thermal behaviour of uncured resin and cured materials was completely different. Moreover, materials with various nanoclay contents showed a different thermal behaviour. The influence of cure temperature (at constant nanoclay content) on the thermal degradation of materials is shown in Fig. 8 (conversion) and Fig. 9 (conversion derivative). It was found that the thermal decomposition of cured materials was independent of cure temperature. The uncured resin presented three zones of maximum degradation rate, with peak temperatures at 197 °C (3.3% conversion), 327 °C (32.7% conversion, the most important peak) and 358 °C (48.9% conversion). Its temperature of thermal stability was $T_5 = 214$ °C. However, when the uncured resin was decomposed in the presence of the hardener, only one peak appeared at 389 °C (35.7% conversion) and the temperature of thermal stability was $T_5 = 344$ °C. In this case, the resin was cured in the thermogravimeter before thermal degradation took place at

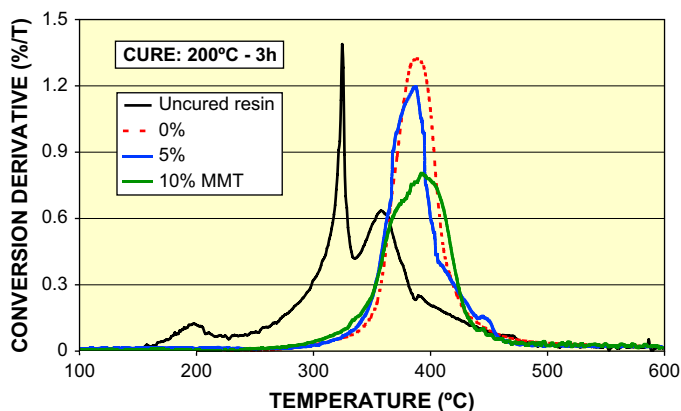


Fig. 7. Variation of the thermal degradation conversion derivative as a function of temperature for uncured resin and materials (containing 0, 5 and 10% of nanoclay) cured at 200 °C for 3 h.

higher temperatures. As expected, when the resin was cured in dynamic conditions (i.e. linear increase of temperature), it became more stable compared to pure resin. In addition, there was only one decomposition zone for cured materials (with and without nanoparticles).

Table 3 contains parameters characterizing the thermal degradation (as a function of the nanoclay content and cure temperature) such as temperature of thermal stability (T_5), temperature T_{50} , temperature at the maximum degradation rate (i.e. peak temperature, T_p), conversion at the peak temperature (α_p) and conversion derivative at the peak temperature ($(d\alpha/dT)_p$). It was found that there was no significant influence of cure temperature and time on these parameters at a given nanoclay content, because of their random oscillation. For this reason, mean values and confidence intervals were calculated for each nanoclay content (0, 5 and 10%). On the contrary, the results clearly showed that the nanoclay content was a variable to be taken into consideration and it had a significant influence on some of thermal parameters, especially when comparing materials with 0 and 10% of nanoclay. Nanocomposites with 5% of nanoclay had a thermal stability ($T_5 = 350 \pm 4$ °C and $T_{50} = 407 \pm 5$ °C) significantly equal

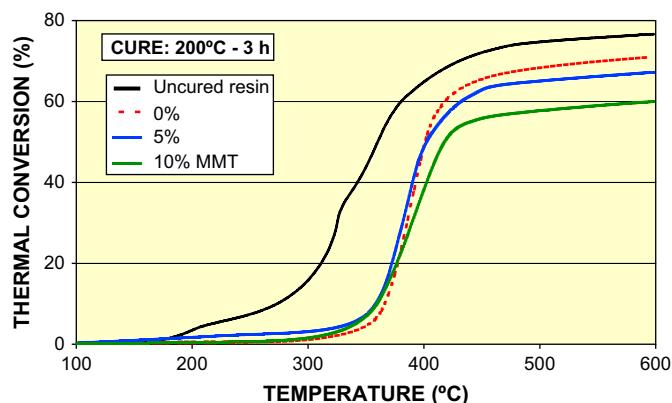


Fig. 6. Variation of the thermal degradation conversion as a function of temperature for uncured resin and materials (containing 0, 5 and 10% of nanoclay) cured at 200 °C for 3 h.

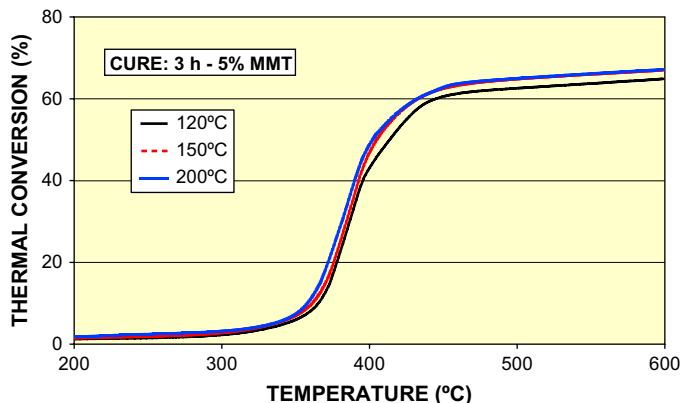


Fig. 8. Variation of the thermal degradation conversion as a function of temperature for nanocomposites (containing 5% of nanoclay) cured at 120, 150 and 200 °C for 3 h.

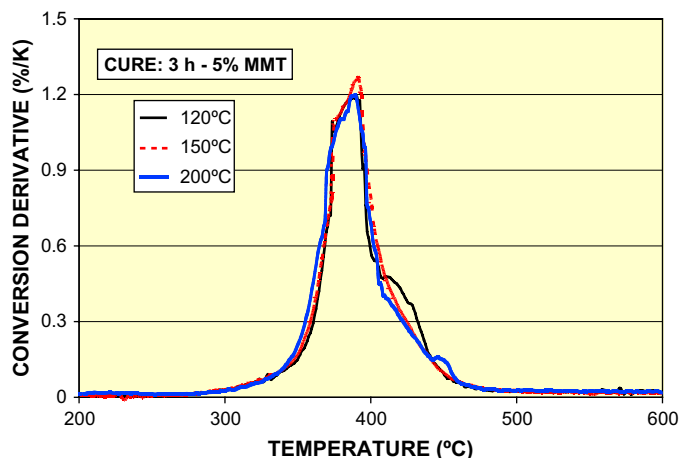


Fig. 9. Variation of the thermal degradation conversion derivative as a function of temperature for nanocomposites (containing 5% of nanoclay) cured at 120, 150 and 200 °C for 3 h.

to that of composites without nanoparticles ($T_5 = 356 \pm 3$ °C and $T_{50} = 404 \pm 3$ °C) as evidenced by the superposition of confidence intervals. However, when the nanoclay content increased up to 10%, the thermal stability was significantly different ($T_5 = 342 \pm 4$ °C and $T_{50} = 415 \pm 3$ °C) compared to that of unfilled materials. The thermal degradation of the nanocomposite with 10% of nanoclay ($T_5 = 342$ °C) starts earlier than that of material without nanoparticles ($T_5 = 356$ °C). On the contrary, when the thermal degradation was already important (i.e. higher conversions), the nanoparticles provided

a certain thermal resistance to the material: $T_{50} = 415$ °C (10% of nanoclay) instead of $T_{50} = 404$ °C (0% of nanoclay). Given that the thermal degradation of the material depends on its composition and chemical structure, the presence of nanoparticles up to 10% is responsible for a certain variation of the thermal stability in comparison with that of composite without nanoparticles. However, there were no significant differences between peak temperatures at the various nanoclay contents under study, which was confirmed by the superposition of the confidence intervals. Even though the differences were not significant, a slight tendency to decrease was observed when increasing the nanoclay percentage (390, 388 and 386 °C for 0, 5 and 10% of nanoclay content, respectively). Again, the conversion at the peak temperature showed no significant difference as a function of nanoclay content, but it was observed a certain decreasing trend (31.8 and 27.7% for 0 and 10% of nanoclay content, respectively). However, there were significant differences in the values of the conversion derivative, being the mean values 1.38, 1.22 and 1.02%/K for 0, 5 and 10% of nanoclay content, respectively.

As it was previously reported in literature [32,33], it is possible to evaluate the activation energy from the thermal parameters determined at the maximum rate of decomposition (i.e. peak temperature, conversion and conversion derivative), using the following equation:

$$E = nRT_p^2 \frac{\left(\frac{d\alpha}{dT}\right)_p}{(1 - \alpha_p)} \quad \forall n$$

Table 3

Thermal stability temperatures and peak temperature, conversion and conversion derivative as a function of cure temperature and time at three nanoclay content levels (confidence intervals at 95% confidence level)

| Cure conditions (°C, h) | T_5 (°C) | T_{50} (°C) | T_p (°C) | α_p (%) | $d\alpha_p/dT$ (%/K) |
|-------------------------|-------------|---------------|-------------|----------------|----------------------|
| <i>0% Nanoclay</i> | | | | | |
| 120, 3 | 355 | 401 | 382 | 26.1 | 1.44 |
| 120, 6 | 354 | 402 | 391 | 37.6 | 1.48 |
| 120, 9 | 358 | 408 | 396 | 36.4 | 1.40 |
| 150, 3 | 359 | 407 | 386 | 25.4 | 1.35 |
| 200, 2 | 356 | 404 | 397 | 41.8 | 1.32 |
| 200, 3 | 352 | 401 | 391 | 38.3 | 1.32 |
| Confidence interval | 356 ± 3 | 404 ± 3 | 390 ± 6 | 34.3 ± 7.2 | 1.38 ± 0.07 |
| <i>5% Nanoclay</i> | | | | | |
| 120, 3 | 343 | 414 | 389 | 32.9 | 1.19 |
| 120, 6 | 348 | 408 | 387 | 32.6 | 1.28 |
| 120, 9 | 349 | 408 | 385 | 29.2 | 1.24 |
| 150, 3 | 350 | 405 | 391 | 38.1 | 1.26 |
| 200, 2 | 356 | 404 | 391 | 32.8 | 1.12 |
| 200, 3 | 352 | 401 | 388 | 37.8 | 1.20 |
| Confidence interval | 350 ± 4 | 407 ± 5 | 388 ± 2 | 33.9 ± 3.6 | 1.22 ± 0.06 |
| <i>10% Nanoclay</i> | | | | | |
| 120, 3 | 341 | 416 | 384 | 26.5 | 1.04 |
| 120, 6 | 344 | 413 | 389 | 33.3 | 1.19 |
| 120, 9 | 347 | 412 | 389 | 33.0 | 1.17 |
| 150, 3 | 340 | 415 | 382 | 32.0 | 0.86 |
| 200, 3 | 340 | 418 | 386 | 27.3 | 0.84 |
| Confidence interval | 342 ± 4 | 415 ± 3 | 386 ± 4 | 30.4 ± 4.1 | 1.02 ± 0.21 |

Moreover, the frequency factor can be also calculated from the thermal parameters determined at the peak temperature, activation energy and heating rate (β), by means of the following equation:

$$A = \beta \frac{\left(\frac{d\alpha}{dT}\right)_p}{(1 - \alpha_p)^n} \exp\left(\frac{E}{RT_p}\right) \quad \forall n$$

Assuming that the decomposition reaction was of first-order (i.e. $n = 1$) and that the conversion was evaluated with respect to the initial organic sample mass, the activation energies were 77.0, 70.5 and 59.2 kJ/mol for the materials containing 0, 5 and 10% of nanoclay, respectively. Therefore, the presence of nanoparticles caused a decrease in the energy necessary to promote the thermal degradation reactions. It was possible to obtain an excellent correlation between the activation energy and the nanoclay content (MMT), which is expressed as follows:

$$E(\text{kJ/mol}) = 77.8 - 1.78 \text{ MMT}(\%) \quad r^2 = 0.976$$

This equation indicates that the activation energy of the thermal decomposition process decreased 17.8 kJ/mol when the nanoclay content increased from 0 to 10%.

Assuming that the decomposition reaction was of first-order, the frequency factors were 4079, 1201 and 128 s⁻¹ for the materials containing 0, 5 and 10% of nanoclay, respectively. Therefore, the frequency factor decreased when increasing the nanoclay content. This means that the collisions responsible for the degradation reactions were less effective when the resin was protected within the nanoclay galleries. Considering the data of frequency factor and those of activation energy, a compensation factor was found between these kinetic parameters, which was expressed by the following correlation:

$$\ln A(\text{s}^{-1}) = -6.6366 + 0.1944E(\text{kJ/mol}) \quad r^2 = 0.9998$$

It was demonstrated that an increase of nanoclay content led to both lower activation energy and frequency factor. It can be explained as follows. The collisions between resin molecules, which are trapped within the nanoclay galleries, were less effective because they were protected against thermal degradation by the galleries. However, once the collision was effective, the thermal activation occurred more readily.

4. Conclusions

As shown by FTIR spectroscopy, there was an asymptotic cure conversion, depending on both cure temperature and nanoclay content: 75–80%, 85–92% and 99–100%, when curing at 120, 150 and 200 °C, respectively. The asymptotic value of conversion was reached at 270–450 min (at 120 °C), 110–140 min (at 150 °C) and 50–70 min (at 200 °C), depending on the nanoclay content (the higher the nanoclay content, the lower the cure time). It was possible to attain similar half-life values at lower temperatures by incorporating nanoparticles (i.e. $t_{1/2} = 22$ –24 min were reached

with the following operating conditions: 150 °C and 5% of nanoclay or 200 °C without nanoclay). Cure reactions were very fast when operating at 200 °C for materials containing 10% of nanoclay (i.e. $t_{1/2} = 10$ min). Nanocomposites with 10% of nanoclay had a thermal stability ($T_5 = 342 \pm 4$ °C) significantly different to that of composites without nanoparticles ($T_5 = 356 \pm 3$ °C). The activation energies of thermal degradation were 77, 70 and 59 kJ/mol for the materials containing 0, 5 and 10% of nanoclay, respectively. It was demonstrated that an increase of nanoclay content led to both lower activation energy and frequency factor. It can be explained as follows: The collisions between resin molecules, which are trapped within the nanoclay galleries, were less effective due to the protection effect of the galleries against thermal degradation. However, once the collision was effective, the thermal activation occurred more readily.

Acknowledgement

We would like to thank Dr. M. Lipinska, visiting Professor at Universitat Politècnica de Catalunya (UPC), for her contribution in the experimental section and T. Lacorte (UPC) for her technical assistance.

References

- [1] Becker O, Simon GP, Varley RJ, Halley P. Layered silicate nanocomposites based on various high-functionality epoxy resins: the influence of an organoclay on resin cure. *Polym Eng Sci* 2004;43(4):850–62.
- [2] Chong KP. Nanoscience and engineering in mechanics and materials. *J Phys Chem Solid* 2004;65(8–9):1501–4.
- [3] Gărea S, Iovu H, Stoleriu S, Voicu G. Synthesis and characterization of new nanocomposites based on epoxy resins and organophilic clays. *Polym Int* 2007;56(9):1106–14.
- [4] Hartwig A, Sebald M, Pütz D, Aberle L. Preparation, characterisation and properties of nanocomposites based on epoxy resins – An overview. *Macromol Symp* 2005;221(1):127–36.
- [5] Jia Q, Zheng M, Cheng J, Chen H. Morphologies and properties of epoxy resin/layered silicate–silica nanocomposites. *Polym Int* 2006;55(11):1259–64.
- [6] Someya Y, Shibata M. Morphology, thermal, and mechanical properties of vinyl ester resin nanocomposites with various organo-modified montmorillonites. *Polym Eng Sci* 2004;44(11):2041–6.
- [7] Triantafyllidis CS, Le Baron PC, Pinnavaia TJ. Thermoset epoxy–clay nanocomposites: The dual role of α,ω -diamines as clay surface modifiers and polymer curing agent. *J Solid State Chem* 2002;167:354–62.
- [8] Xu W, Bao S, He PS. Intercalation and exfoliation behaviour of epoxy resin/curing agent/montmorillonite nanocomposite. *J Appl Polym Sci* 2002;84(4):842–9.
- [9] Zhang K, Wang L, Wang F, Wang G, Li Z. Preparation and characterization of modified-clay-reinforced and toughened epoxy-resin nanocomposites. *J Appl Polym Sci* 2003;91(4):2649–52.
- [10] Carrasco F, Pagès P, Lacorte T, Briceño K. Fourier transform IR and differential scanning calorimetry study of curing a trifunctional amino-epoxy resin. *J Appl Polym Sci* 2005;98(4):1524–35.
- [11] Mustata F, Bicu F. Multifunctional epoxy resins: synthesis and characterization. *J Appl Polym Sci* 2000;77(11):2430–6.
- [12] Becker O, Cheng YB, Russell JV, Simon GP. Layered silicate nanocomposites based on various high-functionality epoxy resins: the influence of cure temperature on morphology, mechanical properties, and free volume. *Macromolecules* 2003;36(5):1616–25.

- [13] Brown JM, Curliss D, Vaia RA. Thermoset-layered silicate nanocomposites. Quaternary ammonium montmorillonite with primary diamine cured epoxies. *Chem Mater* 2000;12(11):3376–84.
- [14] Román F, Montserrat S, Hutchinson JM. On the effect of montmorillonite in the curing reaction of epoxy nanocomposites. *J Therm Anal Calorim* 2007;87(1):113–8.
- [15] Pagès P, Lacorte T, Lipinska M, Carrasco F. Study of curing of layered silicate/trifunctional epoxy nanocomposites by means of FTIR spectroscopy. *J Appl Polym Sci*. doi:10.1002/app.27853.
- [16] Kornmann X, Lindbergh H, Berglund LA. Synthesis of epoxy–clay nanocomposites. Influence of the nature of clay on structure. *Polymer* 2001;42(4):1303–10.
- [17] Kornmann X, Lindbergh H, Berglund LA. Synthesis of epoxy–clay nanocomposites. Influence of the nature of the curing agent on structure. *Polymer* 2001;42(10):4493–9.
- [18] Cañavate J, Pagès P, Saurina J, Colom X, Carrasco F. Determination of small interactions in polymer composites by means of FTIR and DSC. *Polym Bulletin* 2000;44(3):293–300.
- [19] Carrasco F, Pagès P, Pascual S, Colom X. Artificial aging of high-density polyethylene by ultraviolet irradiation. *Eur Polym J* 2001;37(7):1457–64.
- [20] Colom X, Pagès P, Saurina J, Cañavate J, Carrasco F. Changes in crystallinity of the HDPE matrix in composites with cellulosic fibres using DSC and FT-IR. *J Reinf Plast Comp* 2000;19(10):818–30.
- [21] Sánchez-Soto M, Pagès P, Lacorte T, Briceño K, Carrasco F. Curing FTIR study and mechanical characterization of glass bead filled trifunctional epoxy composites. *Comput Sci Technol* 2007;67(9):1974–85.
- [22] Erickson KL. Thermal decomposition mechanisms common to polyurethane, epoxy, poly(diallyl phthalate), polycarbonate and poly(phenylene sulfide). *J Therm Anal Calorim* 2007;89(2):427–40.
- [23] Guinesi LS, da Roz AL, Corradini E, Mattoso LHC, Teixeira EM, Curvelo AS. Kinetics of thermal degradation applied to starches from different botanical origins by non-isothermal procedures. *Thermochim Acta* 2006;447(2):190–6.
- [24] Nakagawa H, Tsuge S, Koyama T. Studies on thermal degradation of epoxy resins by high-resolution pyrolysis-gas chromatography. *J Anal Appl Pyrolysis* 1987;12(2):97–113.
- [25] Núñez L, Fraga F, Castro A, Fraga L. Elastic moduli and activation energies for an epoxy/m-XDA system by DMA and DSC. *J Therm Anal Calorim* 1998;52(3):1013–22.
- [26] Patel RD, Patel RG, Patel VS. Kinetics of thermal degradation of cured epoxy resins based on triglycidyl-*p*-aminophenol. *Thermochim Acta* 1988;128:149–56.
- [27] Ramos-Filho FG, Mélo TJA, Rabello MS, Silva SML. Thermal stability of nanocomposites based on polypropylene and bentonite. *Polym Degrad Stab* 2005;89(3):383–92.
- [28] Rosu D, Cascavaf CN, Ciobanu C, Rosu L. An investigation of the thermal degradation of epoxy maleate of bisphenol A. *J Anal Appl Pyrolysis* 2004;72(1):191–6.
- [29] Soni HK, Patel VS, Patel RG. Studies on cure kinetics and thermal stability of liquid resin based on bisphenol-C and epichlorhydrin using different amines as curing agents. *Thermochim Acta* 1991;191(2):307–16.
- [30] Villanueva M, Fraga I, Rodríguez-Añón JA, Proupín-Castiñeiras J, Martín JL. Study of the influence of water absorption on different epoxy-diamine systems by DSC. *J Therm Anal Calorim* 2007;87(1):205–9.
- [31] Cole KC, Hechler JJ, Noel D. A new approach to modelling the cure kinetics of epoxy/amine thermosetting resins. 2. Application to a typical system based on bis[4-(diglycidylamino)phenyl] methane and bis(4-aminophenyl) sulfone. *Macromolecules* 1991;24(11):3098–110.
- [32] Carrasco F, Pagès P. Thermogravimetric analysis of polystyrene: influence of sample weight and heating rate on thermal and kinetic parameters. *J Appl Polym Sci* 1996;61(1):187–97.
- [33] Carrasco F, Dionisi D, Martinelli A, Majone M. Thermal stability of polyhydroxyalkanoates. *J Appl Polym Sci* 2006;100(3):2111–21.